Influence of different phonon modes on the exciton ground-state energy in a quantum well in an electric field

H. J. Xie
Department of Physics, Guangzhou Teachers' College, Guangzhou 510400, People's Republic of China

C. Y. Chen
Center of Theoretical Physics, China Center of Advanced Science and Technology (World Laboratory), P.O. Box 8730, Beijing 100080, People's Republic of China
*and Department of Physics, Guangzhou Teachers' College, Guangzhou 510400, People's Republic of China**

S. D. Liang
Department of Physics, Guangzhou Teachers' College, Guangzhou 510400, People's Republic of China
(Received 7 November 1994; revised manuscript received 27 February 1995)

The ground-state energy and the binding energy of an exciton in a GaAs/$Ga_{1-x}Al_xAs$ quantum well under an electric field have been studied, and the interactions between excitons and different phonon modes have been taken into consideration. Numerical calculations show that an electric field brings more obvious interface phonon effects and makes the influence of other phonon modes different compared to those without an electric field.

I. INTRODUCTION

In recent years, the properties of Wannier excitons in a quantum well have aroused a great deal of interest,[1-9] because in these kinds of localized semiconductor structures quantum effects make the properties of excitons different from those in three-dimensional systems. Some work has been done on the effect of an electric field on the exciton properties in a quantum well.[1,9] It is understood that the exciton binding energy will be reduced due to the polarization of the exciton wave function by the electric field.[1] As photocurrent technique began to be used in studying the optical properties of quantum wells, the problem of excitons in a quantum well under an external electric field became of practical interest.

The interaction of excitons and optical phonons is an important factor influencing exciton properties in a polar semiconductor structure. Considerable work has been done on the problem of polaron effects in quantum-well structures, both theoretically[4,5,8-14] and experimentally.[15] However, when dealing with polaron effect in quantum-well structures, many authors only consider the bulk longitudinal optical (LO) phonon mode, i.e., they ignore the lattice structural difference between a quantum-well structure and a bulk semiconductor.[5,10,11] It has been proved theoretically and experimentally that interface phonon modes make a great contribution to polaron effects in quantum-well structures.[8,13-15] Hai *et al.*[13] reported a strong polaron effect caused by the interface phonons as the well becomes narrow. Our recently published paper[8] showed that interface phonons and other phonon modes can influence the exciton ground-state energy. The contributions of different phonon modes to the exciton energy shift depend on the well width and the height of the well potential. Certainly, when an electric field is introduced into a quantum-well structure, the well potential will be changed. This will have interesting effects on the exciton-phonon system.

In the present paper, we investigate, the shifts of the exciton ground-state energy and binding energy due to the influence of various phonon modes when the exciton is in a quantum well under an electric field. In order to understand the influence of different phonon modes in detail, different well widths (20–600 Å) and different field strengths (0–120 kV/cm) are considered in our calculation. In the following, the theoretical framework is given in Sec. II. In Sec. III, we give the numerical calculation results and some discussion.

II. THEORY

Consider a GaAs/$Ga_{1-x}Al_xAs$ quantum well (see the Fig. 1). Under the effective-mass approximations the Hamiltonian of the exciton and phonons in a quantum well of width W can be written as [the electric field is applied along the growth axis (z axis) of the well]

$$H=H_{ez}+H_{hz}+\frac{P_x^2+P_y^2}{2M}+\frac{p_x^2+p_y^2}{2\mu}-\frac{e^2}{\varepsilon_\infty\sqrt{\rho^2+(z_e-z_h)^2}}+H_{\rm ph}+H_{\rm int}\ . \tag{1}$$

The first two terms are the Hamiltonians of electrons and holes on the z axis:

$$H_{ez}=-\frac{\hbar^2}{2m_{ez}}\frac{d^2}{dz_e^2}+eFz_e+V_e(z_e)\ , \tag{2}$$

$$H_{hz}=-\frac{\hbar^2}{2m_{hz}}\frac{d^2}{dz_h^2}-eFz_h+V_h(z_h)\ , \tag{3}$$

and for a finite well $V(z)=0$ when $|z|<W/2$ and

 ©1995 The American Physical Society

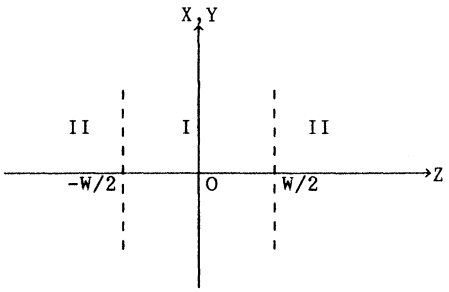

FIG. 1. Geometry of a GaAs/$Ga_{1-x}Al_xAs$ quantum well: I, GaAs; II, $Ga_{1-x}Al_xAs$.

$V(z)=V$ when $|z|>W/2$.

The third and fourth terms in (1) are the kinetic energies of the exciton center of mass and relative motion perpendicular to the z direction. (P_x,P_y) and (p_x,p_y) are the in-xy-plane projection of the exciton center-of-mass momentum and relative motion momentum, respectively. $M=m_e+m_h$ is the total mass of the exciton and $\mu=m_e m_h/(m_e+m_h)$ is the reduced mass of electrons and holes with respect to motion in the xy plane. The fifth term is the Coulomb potential between electron and hole. $H_{\rm ph}$ is the phonon Hamiltonian and $H_{\rm int}$ is the interaction Hamiltonian of the exciton and phonons of various modes.

According to Refs. 16 and 18, there are four types of optical phonon modes interacting with the excitons: (i) symmetric interface optical phonon modes ($S\pm$) with frequency $\omega_{S\pm}(Q)$, (ii) antisymmetric interface optical phonon modes ($A\pm$) with frequency $\omega_{A\pm}(Q)$, (iii) confined slab LO-phonon modes in the well (SL) with frequency ω_{L_1}, and (iv) half-space LO-phonon modes in the barrier layers (HS) with frequency ω_{L_2}.

Then

$$H_{\rm ph}=\sum_{\sigma,\mathbf{Q}}\hbar\omega_\sigma a_\sigma^\dagger(\mathbf{Q})a_\sigma(\mathbf{Q}) , \tag{4}$$

$$H_{\rm int}=\sum_{\sigma,\mathbf{Q}}\{\exp(i\mathbf{Q}\cdot\mathbf{R}) \times[\Gamma_\sigma(Q,z_e)\exp(i\beta_h\mathbf{Q}\cdot\rho)-\Gamma_\sigma(Q,z_h) \times\exp(-i\beta_e\mathbf{Q}\cdot\rho)]a_\sigma^\dagger+\text{H.c.}\} , \tag{5}$$

where σ denotes the phonon mode, $\sigma=$SL,HS, $S\pm$, $A\pm$, $\mathbf{q}=(\mathbf{Q},q_z)$, $\beta_e=m_e/M$, and $\beta_h=m_h/M$.

The dispersion relation for the interface phonon is given by[16]

$$\omega_{l\pm}(Q)=\left[\frac{1}{2(\varepsilon_1^l+\varepsilon_2^l)}\{\varepsilon_1^l(\omega_{L_1}^2+\omega_{T_2}^2)+\varepsilon_2^l(\omega_{L_2}^2+\omega_{T_1}^2) \pm\sqrt{[\varepsilon_1^l(\omega_{L_1}^2+\omega_{T_2}^2)+\varepsilon_2^l(\omega_{L_2}^2+\omega_{T_1}^2)]^2-4(\varepsilon_1^l+\varepsilon_2^l)(\varepsilon_1^l\omega_{L_1}^2\omega_{T_2}^2+\varepsilon_2^l\omega_{L_2}^2\omega_{T_1}^2)}\}\right]^{1/2} , \tag{6}$$

where $\varepsilon_1^l=\varepsilon_{\infty 1}[1-\gamma_l\exp(-QW)]$, $\varepsilon_2^l=\varepsilon_{\infty 2}[1+\gamma_l\exp(-QW)]$, $\varepsilon_{\infty\nu}(\nu=1,2)$ is the light-frequency dielectric constant of material, and ω_{L_ν}, and ω_{T_ν} are the frequencies of longitudinal-optical vibration and transverse optical vibration respectively. $l\equiv S$ and A refers to the symmetric (S) and antisymmetric (A) modes, respectively. $\gamma_S=1$ and $\gamma_A=-1$. Also

$$\Gamma_{l,\pm}(Q,z)=-\left[\frac{2\pi e^2\hbar}{A\omega_{l,\pm}(Q)}\right]^{1/2}\frac{C_{l,\pm}}{Q}\times\begin{cases}\exp[-Q(z-\frac{1}{2}W)] , & z>\frac{1}{2}W ,\\ f_l(Q,z) , & |z|<\frac{1}{2}W ,\\ \gamma_l\exp[Q(z+\frac{1}{2}W)] , & z<-\frac{1}{2}W ,\end{cases} \tag{7}$$

where A is the interface area and

$$C_{l,\pm}=\left[\frac{Q[1+\gamma_l\exp(-QW)]}{2}\right]^{1/2}\left[\frac{[\omega_{T_1}^2-\omega_{l,\pm}^2(Q)]^2[\omega_{T_2}^2-\omega_{l,\pm}^2(Q)]^2}{\varepsilon_1^l(\omega_{L_1}^2-\omega_{T_1}^2)[\omega_{T_2}^2-\omega_{l,\pm}^2(Q)]^2+\varepsilon_2^l(\omega_{L_2}^2-\omega_{T_2}^2)[\omega_{T_1}^2-\omega_{l,\pm}^2(Q)]^2}\right]^{1/2} \tag{8}$$

and

$$f_S(Q,z)=\frac{\cosh(Qz)}{\cosh(\frac{1}{2}QW)} , \tag{9}$$

$$f_A(Q,z)=\frac{\sinh(Qz)}{\sinh(\frac{1}{2}QW)} . \tag{10}$$

The coupling function of a single exciton with the confined slab LO-phonon modes with frequency ω_{L_1} is given by

$$\Gamma_{L_1}^j(Q,z)=-\left[\frac{4\pi\hbar^2\omega_{L_1}\alpha_1}{AW}\left[\frac{2\hbar\omega_{L_1}}{M_1}\right]^{1/2}\right]^{1/2} \times\frac{\sin[q_1^j(z+\frac{1}{2}W)]}{\sqrt{Q^2+(q_1^j)^2}} \tag{11}$$

for $|z|<W/2$ and is zero otherwise. The wave vector of the confined slab LO phonon is (Q,q_1^j), where $q_1^j=j\pi/W$, $j=1,2,\ldots$.

The coupling function of a single exciton with the half-space LO-phonon modes in the barrier material with frequency ω_{L_2} is given by

$$\Gamma_{L_2}=-\left[\frac{4\pi\hbar^2\omega_{L_2}\alpha_2}{V_G}\left[\frac{2\hbar\omega_{L_2}}{M_2}\right]^{1/2}\right]^{1/2} \times\begin{cases}\dfrac{\sin[q_z(z-W/2)]}{\sqrt{Q^2+q_z^2}}, & z>W/2,\\ 0, & |z|<W/2,\\ \dfrac{\sin[q_z(z+W/2)]}{\sqrt{Q^2+q_z^2}}, & z<-W/2,\end{cases} \tag{12}$$

where V_G is the volume of the barrier material. The coupling constant characterizing the electron or hole LO-phonon potential strength is quite small for GaAs and $Ga_{1-x}Al_xAs$.

We may use the Lee-Low-Pines (LLP) variational formalism[12] as we have done in Ref. 8. The two unitary transformation operators are

$$S=\exp\left\{i\left[\mathbf{K}-\sum_{\sigma,\mathbf{Q}}a_\sigma^\dagger(\mathbf{Q})a_\sigma(\mathbf{Q})\right]\cdot\mathbf{R}\right\}, \tag{13}$$

$$U=\exp\left\{\sum_{\sigma,\mathbf{Q}}a_\sigma^\dagger(\mathbf{Q})f_\sigma(Q,\rho)-a_\sigma(\mathbf{Q})f_\sigma^*(Q,\rho)\right\}, \tag{14}$$

where $\hbar\mathbf{K}=\mathbf{P}+\sum_{\sigma,\mathbf{Q}}\hbar\mathbf{Q}a_\sigma^\dagger(\mathbf{Q})a_\sigma(\mathbf{Q})$ is the total momentum of the exciton-phonon system for motion in the xy plane. Then we get the following transformed Hamiltonian (neglecting the interaction related to the emission or absorption of two or more virtual phonons):

$$\mathcal{H}=U^{-1}S^{-1}HSU, \tag{15}$$

$$\mathcal{H}=H_{ez}+H_{hz}+\frac{\hbar^2K^2}{2M}-\frac{e^2}{\varepsilon_\infty\sqrt{\rho^2+(z_e-z_h)^2}}-\frac{\hbar^2}{2\mu}\nabla_\rho^2 +\frac{\hbar^2}{2M}\sum_{\sigma,\mathbf{Q}}(Q^2+u_\sigma^2)a_\sigma^\dagger(\mathbf{Q})a_\sigma(\mathbf{Q}) -\frac{2M}{\hbar^2}\sum_{\sigma,\mathbf{Q}}\frac{|V_\sigma(Q)|^2}{Q^2+u_\sigma^2} +\frac{\hbar^2}{2M}\sum_{\sigma,\mathbf{Q}}\frac{Q^2}{Q^2+u_\sigma^2}|A_\sigma(Q)|^2+\mathcal{H}_1, \tag{16}$$

$$\mathcal{H}_1=-\frac{\hbar\mathbf{K}}{M}\cdot\sum_{\sigma,\mathbf{Q}}\hbar\mathbf{Q}[a_\sigma^\dagger(\mathbf{Q})a_\sigma(\mathbf{Q})+f_\sigma(Q,\rho)a_\sigma^\dagger(\mathbf{Q}) +f_\sigma^*(Q,\rho)a_\sigma(\mathbf{Q})+|f_\sigma(Q,\rho)|^2] +\frac{\hbar^2}{2\mu}\sum_{\sigma,\mathbf{Q}}\frac{i\mathbf{Q}\cdot\nabla_\rho}{Q^2+a_\sigma^2}[a_\sigma^\dagger(\mathbf{Q})A_\sigma^*(Q) +a_\sigma(\mathbf{Q})A_\sigma(Q)], \tag{17}$$

where

$$f_\sigma(Q,\rho)=-\frac{2M}{\hbar^2}\frac{V_\sigma^*(Q,\rho)}{Q^2+u_\sigma^2}, \tag{18}$$

$$\frac{\hbar^2u_\sigma^2}{2M}=\hbar\omega_\sigma, \tag{19}$$

$$V_\sigma(Q,\rho)=\Gamma_\sigma(Q,z_e)\exp(i\beta_h\mathbf{Q}\cdot\boldsymbol{\rho}) -\Gamma_\sigma(Q,z_h)\exp(-i\beta_e\mathbf{Q}\cdot\boldsymbol{\rho}), \tag{20}$$

$$A_\sigma(Q)=\frac{2M}{\hbar^2}[\Gamma_\sigma(Q,z_e)\beta_h\exp(i\beta_h\mathbf{Q}\cdot\boldsymbol{\rho}) +\Gamma_\sigma(Q,z_h)\beta_e\exp(-i\beta_e\mathbf{Q}\cdot\boldsymbol{\rho})]. \tag{21}$$

The eigen wave function of the exciton-phonon system can be written as

$$\Psi=\psi(r)|0\rangle, \tag{22}$$

where $\psi(r)$ is the normalized exciton wave function and $|0\rangle$ represents the normalized vacuum state (the state of no phonon). It satisfies

$$a_\sigma(\mathbf{Q})|0\rangle=0.$$

For the low-temperature limit ($T\to0$ K), the effective Hamiltonian of the system will be

$$H_{\text{eff}}=\langle0|\mathcal{H}|0\rangle =H_{ez}+H_{hz}+\frac{\hbar^2K^2}{2M}-\frac{e^2}{\varepsilon_\infty\sqrt{\rho^2+(z_e-z_h)^2}}-\frac{\hbar^2}{2\mu}\nabla_\rho^2 -\frac{2M}{\hbar^2}\sum_{\sigma,\mathbf{Q}}\frac{|V_\sigma(Q)|^2}{Q^2+u_\sigma^2}+\frac{\hbar^2}{2M}\sum_{\sigma,\mathbf{Q}}\frac{Q^2}{Q^2+u_\sigma^2} \times|A_\sigma(Q)|^2. \tag{23}$$

Consider the finite-barrier quantum-well model of the $GaAs/Ga_{1-x}Al_{1-x}Al_xAs$ material. The confining potentials are $V_{e0}=0.6\times(1.155x+0.37x^2)$ eV for electrons and $V_{h0}=0.4\times(1.155x+0.37x^2)$ eV for holes. The wave function in the z direction for an electron (hole) in the lowest subband is given by[13,19]

$$\psi_1(z)=\begin{cases}B(\zeta)\cos(kz)\exp[-\zeta(z+W/2)], & |z|\le W/2,\\ B(\zeta)\cos(kW/2)\exp[-k_1(|z|-W/2)]\exp[-\zeta(z+W/2)], & |z|>W/2,\end{cases} \tag{24}$$

where $k=\sqrt{2m_1E_l}/\hbar$, $k_1=\sqrt{2m_2(V_0-E_l)}/\hbar$; E_l is determined by the equation

$$\tan\left[\frac{W\sqrt{2m_1E_l}}{2\hbar}\right]=\left[\frac{m_1(V_0-E_l)}{m_2E_l}\right]^{1/2}. \tag{25}$$

The normalized constant $B(\zeta)$ is given by

$$B(\zeta)^2=\frac{2\zeta(k_1^2-\zeta^2)\exp(\zeta W)}{\zeta k_1[\cos(kW)+1]\cosh(\zeta W)+k_1^2[\sinh(\zeta W)+X]+\zeta^2[\cos(kW)+1]\sinh(\zeta W)} \tag{26}$$

with

$$X=\frac{1}{\zeta^2+k^2}[\zeta\cos(kW)\sinh(\zeta W)+k\sin(kW)\cosh(\zeta W)],$$

where ζ is the variational parameter. Using $\psi_1(z)$ and Eqs. (2) and (3), we obtain the lowest subband energy for electrons and holes as

$$E_1(\zeta)=\frac{\hbar^2K_\perp^2}{2m_1}-\langle qFz\rangle \tag{27}$$

with

$$K_\perp^2(\zeta)=(k^2-\zeta^2)+B(\zeta)^2\cos^2(kW/2)k_1\zeta\left[\frac{1}{k_1-\zeta}-\frac{e^{-2\zeta W}}{k_1+\zeta}\right]-B(\zeta)^2e^{-\zeta W}\frac{k\zeta}{k^2+\zeta^2}[k\cos(kW)\sinh(\zeta W)$$
$$-\zeta\sin(kW)\cosh(\zeta W)],$$

$$\langle qFz\rangle=\langle H_F\rangle_+ +\langle H_F\rangle_- +\langle H_F\rangle_0 ,$$

$$\langle H_F\rangle_\pm=\pm\frac{qFB(\zeta)^2\cos^2(kW/2)}{4(k_1\pm\zeta)^2}[(k_1\pm\zeta)W+1],$$

$$\langle H_F\rangle_0=\frac{1}{4\zeta^2}qFB(\zeta)^2e^{-\zeta W}[\sinh(\zeta W)-\zeta W\cosh(\zeta W)+Y],$$

$$Y=-\frac{\zeta^2}{(k^2+\zeta^2)^2}[(k^2-\zeta^2)\cos(kW)\sinh(\zeta W)-2k\zeta\sin(kW)\cosh(\zeta W)]-\frac{kW\zeta^2}{k^2+\zeta^2}\sin(kW)\sinh(\zeta W)$$
$$+\zeta W\cos(kW)\cosh(\zeta W),$$

where $q=-e$ for electrons and e for holes. By minimizing $E_1(\zeta)$ according to ζ, we can obtain ζ's for different electric field strengths.

The exciton wave function is

$$\psi(r)=\psi_{1e}(z_e)\psi_{1h}(z_h)\phi_{1s}(\rho,\gamma), \tag{28}$$

where $\phi_{1s}(\rho,\gamma)$ is the normalized wave function of the ground state of a two-dimensional hydrogenlike atom given by

$$\phi_{1s}(\rho,\gamma)=\sqrt{2/\pi}\gamma e^{-\gamma\rho}, \tag{29}$$

where γ is the variational parameter.

The energy of an exciton is given by

$$E_{1s}(1e,1h)=\min_\gamma\langle\psi(r)|H_{\text{eff}}|\psi(r)\rangle, \tag{30}$$

$$\langle\psi(r)|H_{\text{eff}}|\psi(r)\rangle=E_{1e}(\zeta_e)+E_{1h}(\zeta_h)+\frac{\hbar^2K^2}{2M}+\frac{\hbar^2\gamma^2}{2\mu}$$
$$-\frac{4e^2\gamma^2}{\varepsilon_\infty}\int\int\psi_{1e}^2(z_e)\psi_{1h}^2(z_h)|z_e-z_h|\left\{\frac{\pi}{2}[H_1(2\gamma|z_e-z_h|)-N_1(2\gamma|z_e-z_h|)-1\right\}dz_edz_h+\Delta E, \tag{31}$$

where $H_1(x)$ is the first-order Struve function and $N_1(x)$ is the Neumann function (the second-type Bessel function) of the first order.

$$\Delta E=\sum_\sigma\Delta E_\sigma=\Delta E_{S+}+\Delta E_{S-}+\Delta E_{A+}+\Delta E_{A-}+\Delta E_{\text{SL}}+\Delta E_{\text{HS}} \tag{32}$$

is the exciton ground-state energy shift due to the interaction between the exciton and various phonon modes.

$$\Delta E_{l\pm}=-\frac{2Me^2}{\hbar}\int_0^\infty \frac{C_{l\pm}^2}{Q(Q^2+u_{l\pm}^2)}\left[\left[1-\frac{\beta_e}{\beta_h}\frac{Q^2}{Q^2+u_{l\pm}^2}\right]G_{l\pm,e}^2+\left[1-\frac{\beta_h}{\beta_e}\frac{Q^2}{Q^2+u_{l\pm}^2}\right]G_{l\pm,h}^2 - \frac{16\gamma^3}{(Q^2+4\gamma^2)^{3/2}}\left[\frac{Q^2}{Q^2+u_{l\pm}^2}+1\right]G_{l\pm,e}G_{l\pm,h}\right]\frac{dQ}{\omega_{l\pm}(Q)}\ , \tag{33}$$

where $l=S, A$,

$$G_{S\pm}^2=B(\zeta)^2\cos^2(kW/2)\left[\frac{1}{2(Q+k_1-\zeta)}+\frac{e^{-2\zeta W}}{2(k_1+Q+\zeta)}\right] + \frac{B(\zeta)^2e^{-\zeta W}}{4\cosh^2(QW/2)}\left\{\sinh(\zeta W)/\zeta+\frac{\zeta^2}{k^2+\zeta^2}[\zeta\cos(kW)\sinh(\zeta W)+k\sin(kW)\cosh(\zeta W)] + \frac{\zeta^2}{\zeta^2-Q^2}[\zeta\cosh(QW)\sinh(\zeta W)-Q\sinh(QW)\cosh(\zeta W)] + \frac{1}{\zeta^4-2\zeta^2(Q^2-k^2)+(Q^2+k^2)^2} \times[\zeta(\zeta^2-Q^2+k^2)\cos(kW)\cosh(QW)\sinh(\zeta W)-2kQ\zeta\sin(kW)\sinh(QW)\sinh(\zeta W) + k(\zeta^2+Q^2+k^2)\sin(kW)\cosh(QW)\cosh(\zeta W)-Q(\zeta^2-Q^2-k^2)\cos(kW) \times\sinh(QW)\cosh(\zeta W)]\right\}, \tag{34}$$

$$G_{S\pm}=B(\zeta)^2\cos^2(kW/2)\left[\frac{1}{2k_1+Q-2\zeta}+\frac{e^{-2\zeta W}}{2k_1+Q+2\zeta}\right] + \frac{B(\zeta)^2e^{-\zeta W}}{2\cosh(QW/2)}\left\{\frac{1}{\zeta^2-Q^2/4}\left[\zeta\cosh(QW/2)\sinh(\zeta W)-\frac{Q}{2}\sinh(QW/2)\cosh(\zeta W)\right] + \frac{1}{\zeta^4+2\zeta^2(k^2-Q^2/4)+(k^2+Q^2/4)^2} \times\left[(\zeta^2-Q^2/4+k^2)\cos(kW)\cosh(QW/2)\sinh(\zeta W)-kQ\zeta\sin(kW)\sinh(QW/2)\sinh(\zeta W) + k(\zeta^2+Q^2/4+k^2)\sin(kW)\cosh(QW/2)\cosh(\zeta W) - \frac{Q}{2}(\zeta^2-Q^2/4-k^2)\cos(kW)\sinh(QW/2)\cosh(\zeta W)\right]\right\}, \tag{35}$$

$$G_{A\pm}^2=B(\zeta)^2\cos^2(kW/2)\left[\frac{1}{2(Q+k_1-\zeta)}+\frac{e^{-2\zeta W}}{2(k_1+Q+\zeta)}\right] + \frac{B(\zeta)^2e^{-\zeta W}}{4\sinh^2(QW/2)}\left\{-\frac{\sinh(\zeta W)}{\zeta}-\frac{1}{\zeta^2+k^2}[\zeta\cosh(kW)\sinh(\zeta W)+k\sinh(kW)\cosh(\zeta W)] + \frac{1}{\zeta^2-Q^2}[\zeta\cosh(QW)\sinh(\zeta W)-Q\sinh(QW)\cos(\zeta W)] + \frac{1}{\zeta^4-2\zeta^2(Q^2-k^2)+(Q^2+k^2)^2}[-2kQ\zeta\sin(kW)\sinh(QW)\sinh(\zeta W) + \zeta(\zeta^2-Q^2+k^2)\cos(kW)\cosh(QW)\sinh(\zeta W) + k(\zeta^2+Q^2+k^2)\sin(kW)\cosh(QW)\cosh(\zeta W) - Q(\zeta^2-Q^2-k^2)\cos(kW)\sinh(QW)\cosh(\zeta W)]\right\}, \tag{36}$$

$$G_{A\pm}=B(\zeta)^2\cos^2(kW/2)\left[\frac{1}{2k_1+Q-2\zeta}+\frac{e^{-2\zeta W}}{2k_1+Q+2\zeta}\right]$$
$$+\frac{B(\zeta)^2e^{-\zeta W}}{2\sinh(QW/2)}\left\{\frac{1}{\zeta^2-Q^2/4}\left[-\zeta\sinh(QW/2)\cosh(\zeta W)+\frac{Q}{2}\cosh(QW/2)\sinh(\zeta W)\right]\right.$$
$$+\frac{1}{\zeta^4+2\zeta^2(k^2-Q^2/4)+(k^2+Q^2/4)^2}$$
$$\times\left[kQ\zeta\sin(kW)\cosh(QW/2)\cosh(\zeta W)\right.$$
$$-\zeta(\zeta^2-Q^2/4+k^2)\cos(kW)\sinh(QW/2)\cosh(\zeta W)$$
$$-k(\zeta^2+Q^2/4+k^2)\sin(kW)\sinh(QW/2)\sinh(\zeta W)$$
$$\left.\left.+\frac{Q}{2}(\zeta^2-Q^2/4-k^2)\cos(kW)\cosh(QW/2)\sinh(\zeta W)\right]\right\}, \tag{37}$$

$$\Delta E_{\rm SL}=-\frac{4M\omega_{L1}\alpha_1}{W}\left[\frac{2\hbar\omega_{L1}}{M_1}\right]^{1/2}\sum_j\int_0^\infty\frac{Q\,dQ}{Q^2+u_{\rm SL}^2}\left[\left(1-\frac{\beta_e}{\beta_h}\frac{Q^2}{Q^2+u_{\rm SL}^2}\right)G_{j,e}^2+\left[1-\frac{\beta_h}{\beta_e}\frac{Q^2}{Q^2+u_{\rm SL}^2}\right]G_{j,h}^2\right.$$
$$\left.-\frac{16\gamma^3}{(Q^2+4\gamma^2)^{3/2}}\left[\frac{Q^2}{Q^2+u_{\rm SL}^2}+1\right]G_{j,e}G_{j,h}\right], \tag{38}$$

$$G_j^2=\frac{B(\zeta)^2e^{-\zeta W}}{4[Q^2+(q_1^j)^2]}\left\{\sinh(\zeta W)/\zeta+\frac{1}{k^2+\zeta^2}[\zeta\cos(kW)\sinh(\zeta W)+k\sin(kW)\cosh(\zeta W)]\right.$$
$$-\frac{1}{(q_1^j)^2+\zeta^2}\{\zeta e^{\zeta W}/2+[q_1^j\sin(2q_1^jW)-\zeta\cos(2q_1^jW)/2]e^{-\zeta W}\}$$
$$+\frac{1}{\zeta^4+2\zeta^2[k^2+(q_1^j)^2]+[(q_1^j)^2-k^2]^2}$$
$$\times\left[\zeta kq_1^j\sin(kW)\sin(2q_1^jW)e^{-\zeta W}-\frac{\zeta}{2}[\zeta^2+k^2+(q_1^j)^2]\cos(kW)[e^{\zeta W}-\cos(2q_1^jW)e^{-\zeta W}]\right.$$
$$-\frac{k}{2}[\zeta^2+k^2-(q_1^j)^2]\sin(kW)[e^{\zeta W}+\cos(2q_1^jW)e^{-\zeta W}]$$
$$\left.\left.-\frac{q_1^j}{2}[\zeta^2-k^2+(q_1^j)^2]\cos(kW)\sin(2q_1^jW)e^{-\zeta W}\right]\right\}, \tag{39}$$

$$G_j=\frac{B(\zeta)^2e^{-\zeta W}}{2\sqrt{Q^2+(q_1^j)^2}}\left\{\frac{1}{4\zeta^2+(q_1^j)^2}\{q_1^je^{\zeta W}-[q_1^j\cos(q_1^jW)+2\zeta\sin(q_1^jW)]e^{-\zeta W}\}\right.$$
$$+\frac{1}{\zeta^4+2\zeta^2[k^2+(q_1^j)^2/4]+[(q_1^j)^2/4-k^2]^2}$$
$$\times\left[\frac{q_1^j}{4}[\zeta^2-k^2+(q_1^j)^2/4]\cos(kW)[e^{\zeta W}-\cos(q_1^jW)e^{-\zeta W}]\right.$$
$$+\frac{\zeta kq_1^j}{2}\sin(kW)[e^{\zeta W}+\cos(q_1^jW)e^{-\zeta W}]-\frac{\zeta}{2}[\zeta^2+k^2+(q_1^j)^2/4]\cos(kW)\sin(q_1^jW)e^{-\zeta W}$$
$$\left.\left.+\frac{k}{2}[\zeta^2+k^2-(q_1^j)^2/4]\sin(kW)\sin(q_1^jW)e^{-\zeta W}\right]\right\}, \tag{40}$$

$$\Delta E_{\rm HS}=-2M\omega_{L2}\alpha_2\left[\frac{2\hbar\omega_{L_2}}{M_2}\right]^{1/2}\int_0^\infty\frac{Q\,dQ}{Q^2+u_{\rm HS}^2}\left[\left[1-\frac{\beta_e}{\beta_h}\frac{Q^2}{Q^2+u_{\rm HS}^2}\right]G_{\rm HS,e}^2+\left[1-\frac{\beta_h}{\beta_e}\frac{Q^2}{Q^2+u_{\rm HS}^2}\right]G_{\rm HS,h}^2\right], \tag{41}$$

$$G_{\rm HS}^2=\tfrac{1}{4}B(\zeta)^2\cos^2(kW/2)\frac{1}{(k_1-\zeta)(k_1-\zeta+Q)}\ . \tag{42}$$

TABLE I. Material parameters (Refs. 13 and 17).

	GaAs ($\nu=1$)	$Ga_{1-x}Al_xAs$ ($\nu=2$)	AlAs
$m_{\nu,e}$ (units of m_0)	0.067	$0.067+0.083x$	0.15
$m_{\nu,hz}$ (units of m_0)	0.45	$0.45+0.31x$	0.76
$m_{nu,lz}$ (units of m_0)	0.088	$0.088+0.049x$	0.137
$\hbar\omega_{L_\nu}$ (meV)	36.25	$36.25+3.83x+17.12x^2-5.11x^3$	50.09
$\hbar\omega_{T_\nu}$ (meV)	33.29	$33.29+10.70x+0.03x^2+0.86x^3$	44.88
$\varepsilon_{0\nu}$	13.18	$13.18-3.12x$	10.06
$\varepsilon_{\infty\nu}$	10.89	$10.89-2.73x$	8.16

III. RESULTS AND DISCUSSION

A. Exciton energy shift

With the ground-state energy of the exciton-phonon system obtained, we will carry out a numerical calculation for a GaAs/$Ga_{1-x}Al_xAs$ quantum well. The material parameters chosen are the same as those we use in Ref. 8; they are listed in Table I.

The calculation will be carried out on the ground-state energy of the heavy-hole exciton. The Al concentration is $x=0.3$. The heavy-hole effective mass for motion in the x-y plane is $m_{hxy}=(\frac{1}{4}m_{hz}+\frac{3}{4}m_{lz})m_0$, where m_0 is the free-electron mass. Different well widths and different electric field strengths are considered in the calculation.

In Fig. 2, we plotted the exciton ground-state energy shift (ΔE) due to the exciton-phonon interaction as a function of the well width. The electric field strength is fixed: $F=60$ kV/cm. For comparison, the results obtained in the absence of electric field from Ref. 8 are also plotted in the same figure. One can easily conclude that when the electric field is introduced into the system the contributions of different phonon modes to ΔE undergo the same tendency of change as those without electric field as the well width increases. But different modes behave differently under the field. The contribution of the slab LO-phonon mode ($\Delta E_{\rm SL}$) becomes a little bit smaller. This can be understood because the electric field draws electrons and holes in different directions and moves them near the well edges; small portions of the electron and hole wave functions escape out of the well and are beyond the influence of the slab LO-phonon mode. This same reason makes the contribution of the half-space LO-phonon mode ($\Delta E_{\rm HS}$) become greater in comparison with that in the absence of electric field. Figure 3 shows the response to electric field strength with fixed, well width $W=100$ Å. We can see that $|\Delta E_{\rm SL}|$ is reduced and $|\Delta E_{\rm HS}|$ increases as the field strength increases.

Now let us see the contribution of the interface phonon mode ($\Delta E_{\rm in}=\Delta E_{S+}+\Delta E_{S-}+\Delta E_{A+}+\Delta E_{A-}$). It is a little bit greater than that without electric field, because

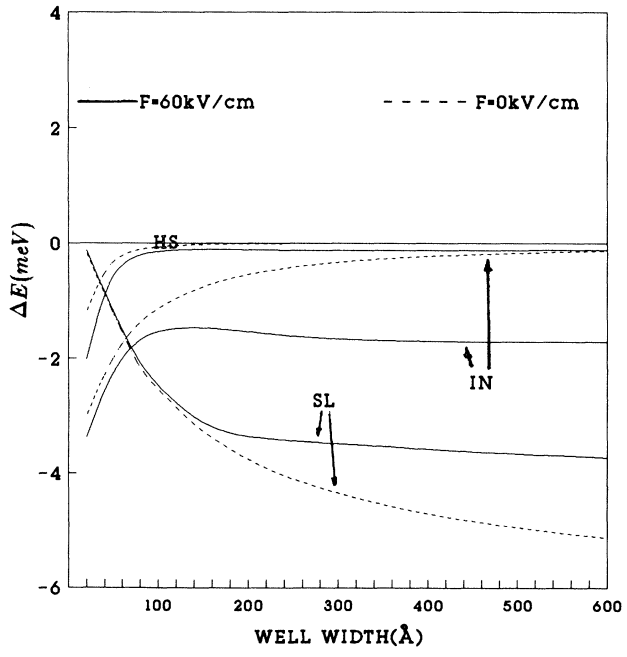

FIG. 2. The exciton ground-state energy shift caused by different phonon modes as a function of the well width.

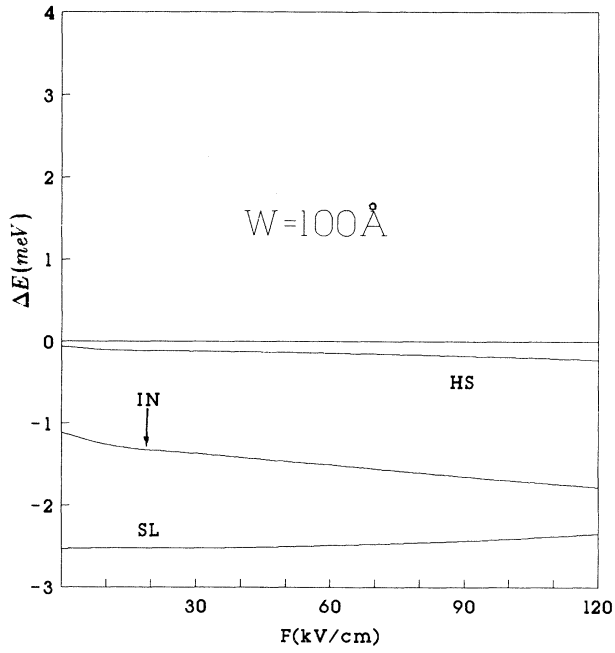

FIG. 3. The exciton ground-state energy shift caused by different phonon modes as a function of the field strength.

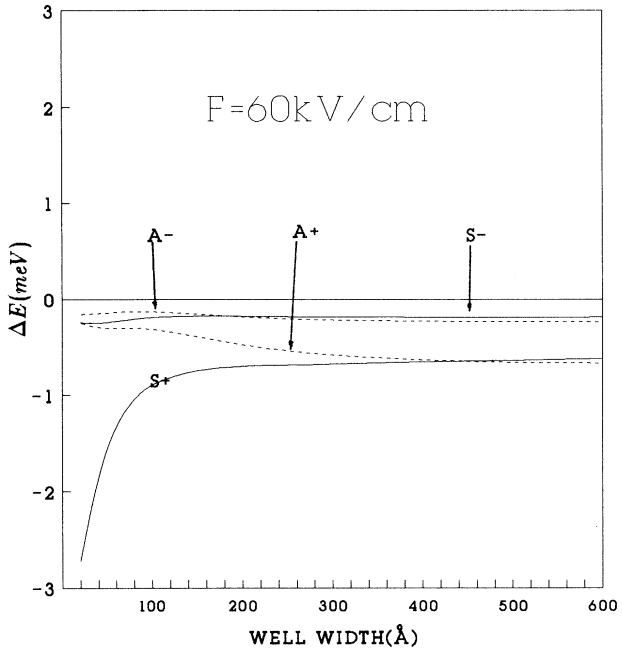

FIG. 4. The contribution to the energy shift of different interface phonon modes as a function of the well width.

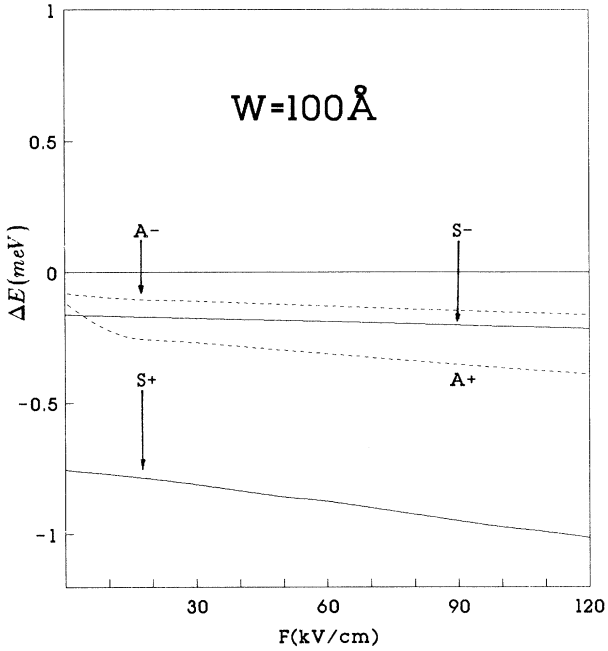

FIG. 5. The contribution to the energy shift of different interface phonon modes as a function of the field strength.

the electron and hole wave functions are near the interface. But when the well width is greater than 150 Å, it does not decrease to zero with increasing well width as it does when there is no electric field (Fig. 2). For a wider well, the same electric field strength modifies the well potential more obviously than it does for a narrower well. So the exciton will have a greater radius under an electric field, and the electron and hole will be driven much closer to the well edges. This will certainly make ΔE_{in} much greater than in the absence of electric field. However, for a wide well, $|\Delta E_{\text{in}}|$ is still much smaller than for a narrow well ($W < 100$ Å). $|\Delta E_{\text{in}}|$ increases as the electric field strength increases (Fig. 3). Careful analysis of ΔE_{in} gives more interesting results. Among the four interface phonon modes, ΔE_{S+} is the major term in ΔE_{in} (Figs. 4 and 5); $|\Delta E_{S-}|$ is small and $|\Delta E_{A\pm}|$ are very small in the absence of electric field. An external electric field breaks the symmetry of the well potential and, of course, the electron and hole wave functions are no longer symmetrical. These make $|\Delta E_{A\pm}|$ become greater. The increase of $|\Delta E_{A\pm}|$ with increasing well width under an electric field (Fig. 4) explains the effect of the well potential asymmetry on $\Delta E_{A\pm}$.

B. Exciton binding-energy shift

It would be more interesting to observe how the exciton binding energy is influenced by the different phonon modes. With the theoretical result obtained above, we calculate the polaron energy shifts for the lowest subband of an electron and a hole. For simplicity, we only give the numerical result [Figs. 6(b) and 6(c)]. The curves in Fig. 6(b) and 6(c) are reasonable according to our previous analysis. With the polaron energy shifts available, the exciton binding-energy shift can be calculated from $\Delta E^B = \Delta E^e + \Delta E^h - \Delta E^{\text{ex}}$. Figure 6(a) shows how ΔE^B changes as the well width increases when there is electric field. The result in the absence of the electric field is also plotted in the same figure for comparison. In Fig. 6(a), we notice that polaron effects caused by different phonon modes influence the exciton binding energy quite differently. The polaron effect may increase the exciton binding energy or reduce it.[5,10,11] This depends on the exciton band mass and the phonon mode. First let us take a look at the interface phonon mode. $|\Delta E^B_{\text{in}}|$ is small when the well is very narrow because the exciton is confined in the well, and the polaron energy shifts for exciton and bound exciton have little difference. As the well grows wider, this difference becomes bigger; it decreases again as the well becomes even wider because the influence of the interface phonon is no longer strong. $|\Delta E^B_{\text{in}}|$ is smaller when there is an electric field. It should be noted that in the absence of electric field the interface phonon tends to "trap" single electrons or holes and keeps part of its influence even when the well is very wide. But for an exciton, the Coulomb force is strong enough to keep it away from the well edges when the well is wide (Fig. 2). This make $|\Delta E^e_{\text{in}}| + |\Delta E^h_{\text{in}}|$ greater than $|\Delta E^{\text{ex}}_{\text{in}}|$ and gives a certain $|\Delta E^B_{\text{in}}|$ for a wide well [Fig. 6(a)]. An external electric field makes the exciton radius greater and the interface phonon has a stronger influence on the exciton energy (Fig. 2). This results in a smaller $|\Delta E^B_{\text{in}}|$ because the "trap" effect for a single electron or hole no longer prevails. The curve of ΔE^B_{SL} is easy to explain since, as we mentioned previously, the electric field reduces $|\Delta E^e_{\text{SL}}|$, $|\Delta E^h_{\text{SL}}|$, and $|\Delta E^{\text{ex}}_{\text{SL}}|$ [Figs. 2, 6(b), and 6(c)].

In conclusion, we have investigated the exciton-

phonon system in a quantum well under an external electric field. Special attention has been paid to the various phonon modes in the quantum-well structure. By using the generalized LLP formalism, we obtained the effective Hamiltonian of the exciton-phonon system. Numerical calculation shows that external electric field will enhance the influence of the interface phonons and LO phonons of the barrier material on the exciton ground-state energy, while the influence of LO phonons in the well material on the exciton ground-state energy is slightly weakened by the electric field. However, the dependence of ΔE_σ on the well width is still similar to that without an electric field. When we turn our attention to the exciton binding energy, a similar conclusion is obtained for the influence

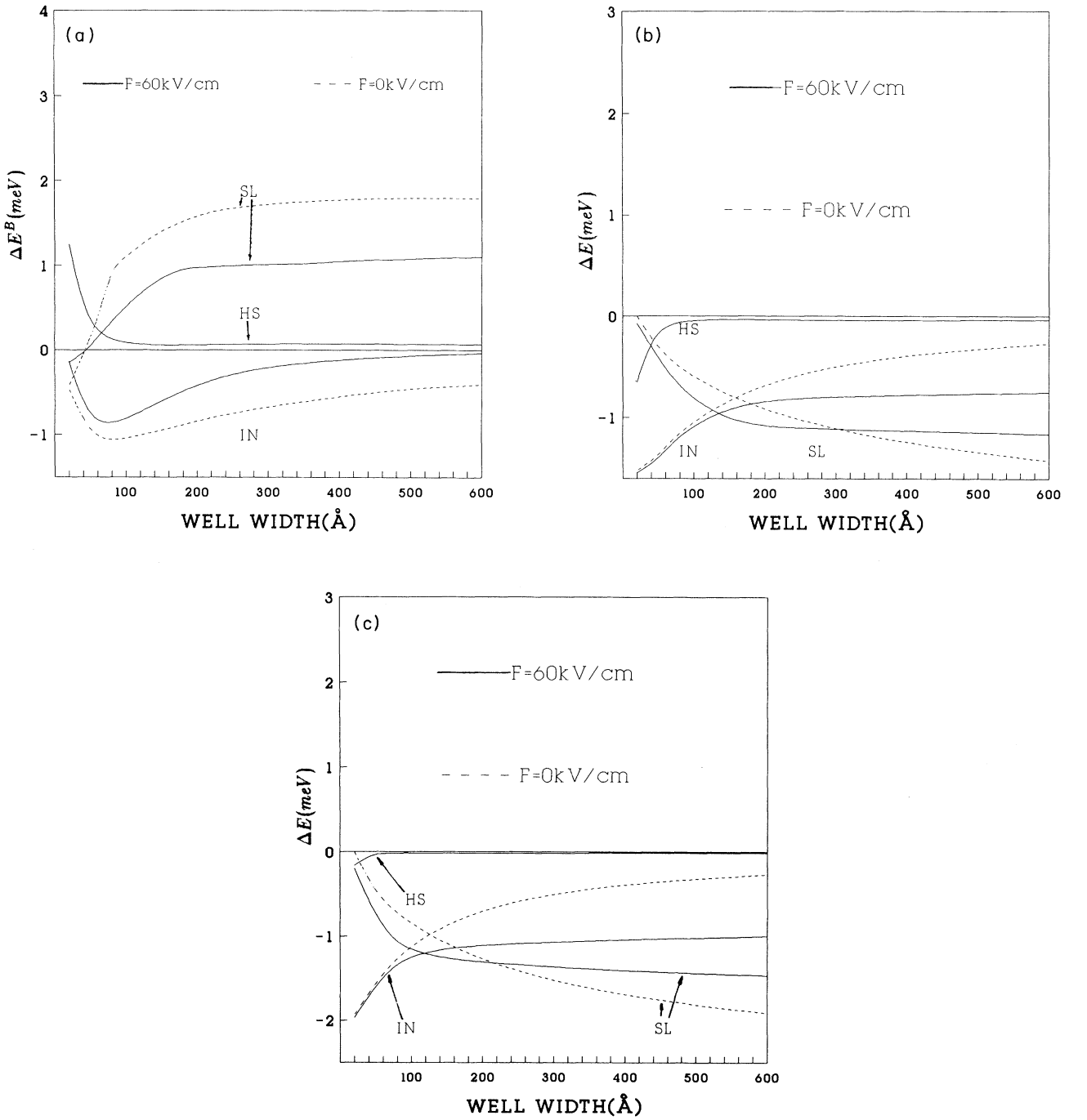

FIG. 6. (a) The exciton binding energy shifts as a function of the well width. (b) The polaron energy shift of an electron. (c) The polaron energy shift of a hole.

of LO phonons in the well material. Unexpectedly, the external electric field, instead of enhancing the influence of interface phonons on the exciton binding energy, will weaken it.

ACKNOWLEDGMENT

This work was supported by the Guang Dong Advanced Educational Bureau, China.

*Mailing address.

[1]J. A. Brum and G. Bastard, Phys. Rev. B **31**, 3893 (1985).
[2]R. L. Green, K. K. Bajaj, and D. E. Phelps, Phys. Rev. B **29**, 1807 (1984).
[3]R. L. Green and K. K. Bajaj, Phys. Rev. B **31**, 6498 (1985).
[4]S. W. Gu and M. Y. Shen, Phys. Rev. B **35**, 9817 (1987).
[5]M. Matsuura, Phys. Rev. B **37**, 6977 (1988).
[6]M. J. L. S. Haines *et al.*, Phys. Rev. B **43**, 11 944 (1991).
[7]X. Zhang and K. K. Bajaj, Phys. Rev. B **44**, 10 913 (1991).
[8]H. J. Xie and C. Y. Chen, J. Phys. Condens. Matter **6**, 1007 (1994).
[9]J. L. Zhu, D. H. Tang, and J. J. Xiong, Phys. Rev. B **39**, 8609 (1989).
[10]Marcos H. Degani and Oscar Hipólito, Phys. Rev. B **35**, 4507 (1987).
[11]Z. G. Koinov, J. Phys. Condens. Matter **3**, 6313 (1991).
[12]T. D. Lee, F. E. Low, and D. Pines, Phys. Rev. **90**, 297 (1953).
[13]G. Q. Hai, F. M. Peeters, and J. T. Devreese, Phys. Rev. B **42**, 11 063 (1990).
[14]C. Y. Chen, S. D. Liang, and M. Li, J. Phys. Condens. Matter **6**, 1903 (1994).
[15]J. P. Cheng, B. D. McCombe, G. Brozak, and W. Shaff, Phys. Rev. B **48**, 17 243 (1993).
[16]N. Mori and T. Ando, Phys. Rev. B **40**, 6175 (1989).
[17]D. S. Chuu and Y. C. Lou, Phys. Rev. B **43**, 14 504 (1991).
[18]R. Chen, D. L. Lin, and T. F. George, Phys. Rev. B **41**, 1435 (1990).
[19]E. E. Mendez, G. Bastard, L. L. Chang, L. Esaki, H. Morkoc, and R. Fischer, Phys. Rev. B **26**, 7101 (1982); Physica B **117&118**, 711 (1983).